

Measurement and Characterization of the Near-Ground Indoor Ultra Wideband Channel

A. Hugine, H. I. Volos, J. Gaedert, R. M. Buehrer
Virginia Polytechnic Institute and State University
466 Whittemore Hall, Blacksburg, VA 24061, USA
E-mail: {ahugine, hvolos, jgaedder, buehrer}@vt.edu

Abstract—The propagation of near-ground indoor ultra-wideband channel is an important issue with significant impacts on the future direction and scope of ultra wideband (UWB) technology and its applications. Near-ground applications are effective where the use of scatter nodes/devices is used in a conventional application, such as rescue personnel. The goal of this article is to present an assessment and characterization of near-ground UWB channels and the potential for near-ground communication systems. Time-domain measurements for UWB indoor propagation channels were taken with transmit and receive antennas placed directly on the ground in order to characterize statistical properties of the channel's impulse response. Both large- and small-scale models were evaluated and compared to existing results for above-ground measurements. The model parameters that were extracted from measurements prove to be in accordance with expected physical trends from previous work. These preliminary results could be advantageous in the design of future near-ground indoor UWB systems capable of fusing propagation and communication functionalities.

I. INTRODUCTION

Ultra-wideband (UWB) technology has recently attracted increasing amount of attention [1]. UWB systems are often defined to have a fractional bandwidth larger than 20 percent of center frequency and/or an absolute bandwidth of more than 500 MHz [2]. Having emerged as one of the most promising technologies for many indoor communication applications, UWB has been proposed for use in such systems as position location devices for rescue personnel, wireless personal area network, and security systems [3]. The development of indoor communication systems requires the availability of sample measurement data in various environments in order to characterize the UWB propagation behavior. Understanding the characteristics of indoor UWB channels is essential for its transceiver design and evaluating its performance.

The channel multipath propagation characteristics are investigated by examining the power delay profiles (PDP), path loss, shadowing, and local fading. It has been found that in UWB channels, the appearance of multipath components are in the forms of disperse, single dominant and clustered paths, their appearance highly dependent upon the measurement environment. UWB systems are robust to multipath fading due to the high multipath diversity gain it has. Channel measurements and modeling are therefore a basic necessity for system design. It has been shown by theoretical as well as practical investigations that UWB channels have properties

that can be fundamentally different than those of the traditional wideband channels [4].

In recent years significant amounts of data have been gathered [2], [5]–[8] to investigate the effects of different environments on UWB propagation, however with the exception of [1], [9] few results exist on the effects of placing transmit and receive antennas on or near the ground. UWB near-ground channels serve as a key component in establishing scatter node systems, where near ground close range RF propagation conditions arise in wireless sensor networks. Near-ground UWB channels are essential aspects of research for various defense organizations; border patrol and homeland security applications require wireless sensor networks positioned on the ground [10]. Wireless sensor networks aim to interface the analog physical world with existing communication and data networks. The radio environment for this kind of wireless RF transmission consists of small range propagation with very low elevation antennas. This serves as an important aspect of near ground UWB channels, due to the fact that lowering the antenna elevation, as our results show, shrinks the range of the entire system, which allows a higher path loss for the wireless network.

In this paper we present time-domain measurements of the indoor near-ground UWB channel and determine channel characteristics from the data. The indoor measurements were performed in typical office/building environments where the transmit (Tx) and receive (Rx) antennas were positioned on the ground at a variety of locations. The following sections compare the near-ground (NG) to above-ground (AG) measurements whose increased path loss, shadowing variance, and local variation are consistent with previous work on the subject [2].

II. MEASUREMENT PROCEDURE

All measurements were performed inside two modern engineering buildings on the campus of Virginia Tech. The antennas were placed on the ground in a variety of rich multipath environments such as corridors, hallways, classrooms, large office rooms, and atriums. The antennas were directly placed on the concrete floor, covered by either tile or carpet. Reference measurements for both were taken, however the effects of carpeting versus tile were found to be negligible.

The experiments were conducted by transmitting a unmodulated baseband 200ps Gaussian pulse from a PicoSecond

10,070A pulse generator directly into a bicone antenna at a pulse rate of 100kHz with an approximate instantaneous Tx power of 25dBm. A Tektronix CSA 8000B digital oscilloscope received the signal from an identical bicone with a 12.5ps sampling resolution over a 50ns window (it was observed that very little multipath energy existed beyond an excess delay of 50ns) while averaging over 200 samples to reduce noise. The receive antenna was placed at various positions on a 90cm 7x7 square grid, as shown in Figure 1, with the number of recorded data points (3x3 or 7x7) being determined by spatial correlation of the received signal. The entire grid was then positioned at a number of locations such that an appropriate path loss model could be generated.

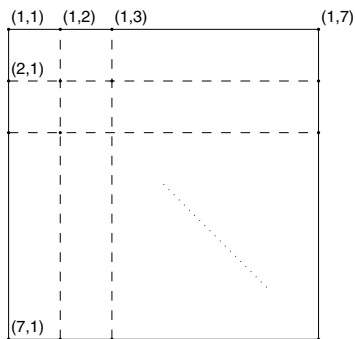


Fig. 1. Grid Layout

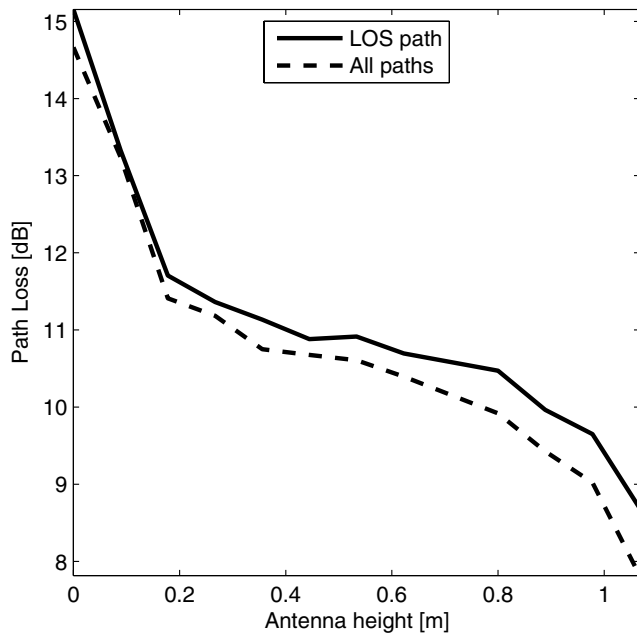


Fig. 2. Path loss as antennas are lowered to the ground. Antennas were lowered together upon non-metallic surfaces with a Tx/Rx separation of 2m.

III. DATA ANALYSIS

To mitigate noise and interference all received signals were filtered with an FIR band-pass filter (0.5 to 12GHz) to remove a low-frequency ringing component due to the antenna and to

remove high-frequency out-of-band noise. Additionally, power below four standard deviations of the noise was neglected. Further data interpretation can be broken into two sections: large scale modeling, which examines the statistics of the entire received power delay profile (PDP) including path loss, shadowing, and local fading, and small-scale time statistics, which investigate the time distribution of energy throughout the received channel impulse response (CIR) including root mean-square delay spread, mean excess delay, and the number of discrete multipath components. Additionally, some measurements were taken to investigate the effects of directly lowering the antennas on the received signal power.

A. Path Loss, Shadowing, and Local Spatial Fading

Path loss, a fundamental characteristic of electromagnetic wave propagation, is useful in communication system design and is often used for link budget calculation and determining transceiver ranges. At a Tx/Rx separation of d , the average path loss is modeled as

$$\bar{P}L(d) = PL_0 + n10 \log_{10} \left(\frac{d_0}{d} \right) \quad (1)$$

where PL_0 is the nominal path loss at a reference measurement d_0 . For all analysis, a 1m Tx/Rx separation measurement was used as reference. The path loss exponent can be estimated from statistical inference of measured data [11]. Typical value of the path loss exponent are $n = 2$ for free space LOS propagation, but UWB channels have been found to have path loss exponents lower than 2 [12], especially for multipath-rich indoor environments where additional energy from disperse multipath components combined at the receiver can be distinctly separated. The values for n in Figure 3 were found by fitting the data via linear regression in the minimum mean-square error sense.

Variations of received power about the average path loss are described as shadowing. Classically modeled with a log-normal distribution having a mean of 0dB and a standard deviation σ_s , shadowing is generally a result of obstructions (such as mountains and civil structures) between transmitter and receiver blocking the LOS component in long-range channels. UWB channels exhibit similar trends, particularly when the LOS path is blocked. Therefore the previous path loss model in (1) can be extended to account for shadowing deviation, viz.,

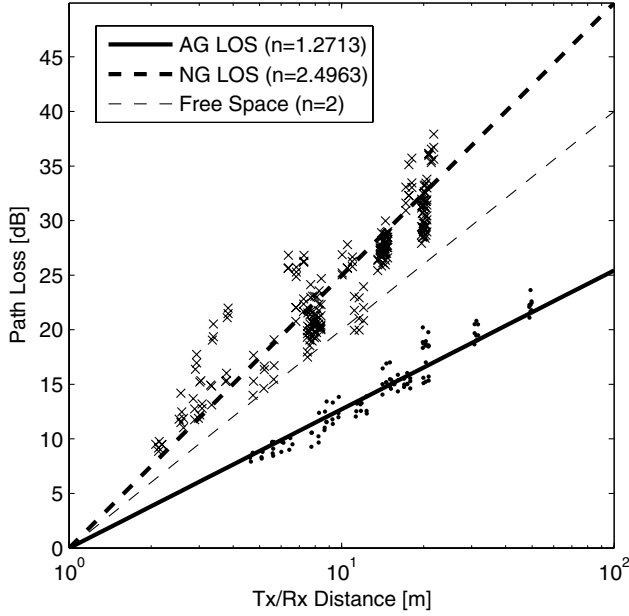
$$PL(d) = PL_0 + n10 \log_{10} \left(\frac{d_0}{d} \right) + X_{\sigma} \quad (2)$$

where X_{σ} is a random variable in decibels which takes on a Gaussian distribution with zero mean. Its standard deviation, σ_s , is calculated directly from the measured variation of the received power about $\bar{P}L(d)$ described in (1). Although some models account for the dependency σ_s has upon Tx/Rx separation, the finite amount of data limited our analysis of σ_s to a static value. The cumulative distribution functions (CDFs) of shadowing statistics are plotted in Figure 4.

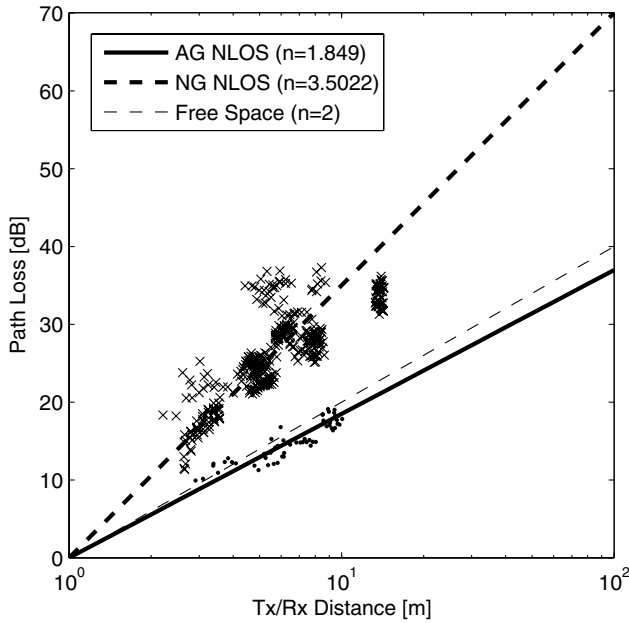
Fading is the variation of power when multipath components combine at the receiver and is generally detrimental

TABLE I
SALEH-VALENZUELA CHANNEL MODEL PARAMETERS

	Above-ground		Near-ground	
	LOS	NLOS	LOS	NLOS
$1/\Lambda$ (ns)	8.1	2	4	9
$1/\lambda$ (ns)	0.25	0.25	0.5	0.25
Γ (ns)	20	25	18	20
γ (ns)	1.7	1	1.5	1.6
σ (dB)	4.5	7	4.5	5



(a) LOS



(b) NLOS

Fig. 3. Relative path loss model for above- and near-ground antenna positions as well as LOS and NLOS scenarios.

to the performance of narrowband systems. If the channel is stationary (which is the assumption for all our analyses), this phenomenon could be observed in a narrowband system by moving the receive antenna a small distance—on the order of a few wavelengths—and re-evaluating the received power. This effect is mitigated as the signal bandwidth increases [13] as in UWB communications systems, but still exists. The issue of local power variation is therefore one which should be addressed.

The analysis of local fading used in this paper assumes the path loss model from (1) adopts a log-normal distribution similar to that of shadowing. The average linear power over the m^{th} grid was calculated as

$$\bar{P}_r^{(m)}(\bar{d}) = \frac{1}{IJ} \sum_{i=1}^I \sum_{j=1}^J \left[\frac{1}{T} \int_0^T |r_{i,j}^{(m)}(t)|^2 dt \right] \quad (3)$$

where $T = 50ns$ is the observation time, and $r_{i,j}^{(m)}(t)$ is the received time-varying signal for the i^{th} of I rows and j^{th} of J columns for the m^{th} grid at an average grid Tx/Rx distance \bar{d} . Note that I and J could be either 3 or 7, as discussed in Section II. The deviation of received power from (3) is

$$\zeta_{i,j}^{(m)} = \left(\frac{d_0 \bar{d}^{(m)}}{\hat{d}_{i,j}^{(m)}} \right)^n \bar{P}_{i,j}^{(m)} \quad (4)$$

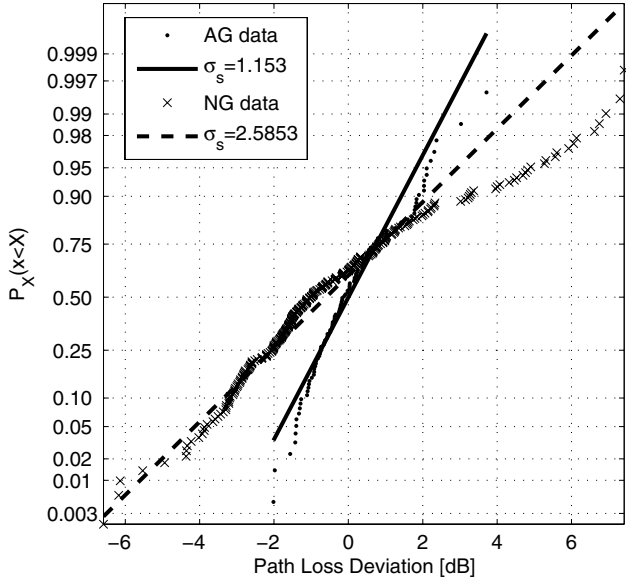
where $\hat{d}_{i,j}^{(m)}$ is the distance between the transmitter and the exact receiver location and n is the path loss exponent determined by (3). One could think of (4) as simply the deviation of the received power from the average grid power, compensated by the small variation in Tx/Rx distance from point to point on the grid. Assuming a normal distribution in decibels, the fading variance is simply $\sigma_f^2 = E \left\{ [10 \log_{10}(\zeta)]^2 \right\}$ over all i, j , and m . The resulting CDFs are plotted in Figure 5. It is apparent from the figure that the log-normal model is a good fit to the data for both LOS and NLOS cases, with a small amount of variation in received power about the grid.

B. Small Scale Channel Modeling

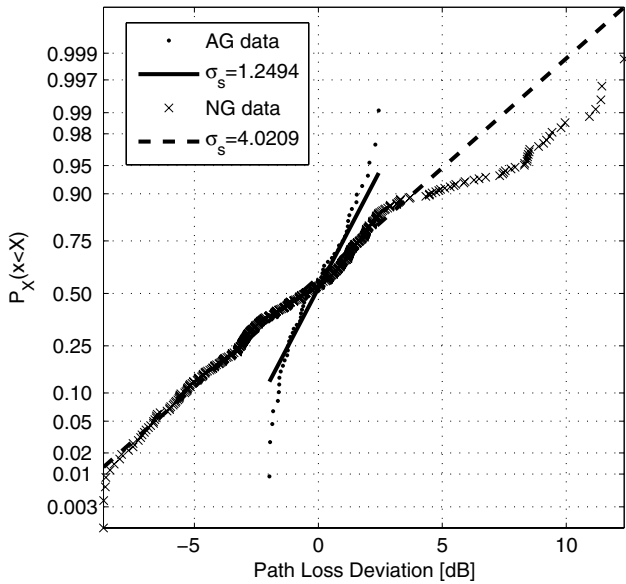
Small scale models describe the effects of received energy distribution throughout a fixed observation time window, often assuming a discrete number of received paths. For analysis of statistics based upon discrete components it is necessary to collapse the received PDPs into discrete time paths, called the channel impulse response (CIR). Because measurements were observed in the time domain, the CLEAN algorithm was

TABLE II
AVERAGE CHANNEL STATISTICS

	Above-ground		Near-ground	
	LOS	NLOS	LOS	NLOS
n	1.27	1.85	2.50	3.50
σ_s (dB)	1.15	1.25	2.59	4.02
σ_f (dB)	0.217	0.565	1.13	1.16
$\bar{\tau}_{rms}$ (ns)	6.30	10.4	8.77	11.2
$\bar{\tau}_m$ (ns)	7.71	15.3	10.4	19.0
N_p	56	114	58	86



(a) LOS



(b) NLOS

Fig. 4. Cumulative distributions of shadowing variations about the mean path loss model and their fits to log-normal distributions.

used to deconvolve the received signal with a $1m$ reference pulse. The CLEAN algorithm is a cross-correlation subtraction method which works well for visually identifiable separate paths, but often can mistake several paths close together in time as just one. The interested reader can read more about the CLEAN algorithm in [12].

For all time statistics this paper adopts a finite stationary linear tap delay line for modeling the CIR, viz.,

$$h(\tau) = \sum_k \beta_k \delta(\tau - \tau_k) \quad (5)$$

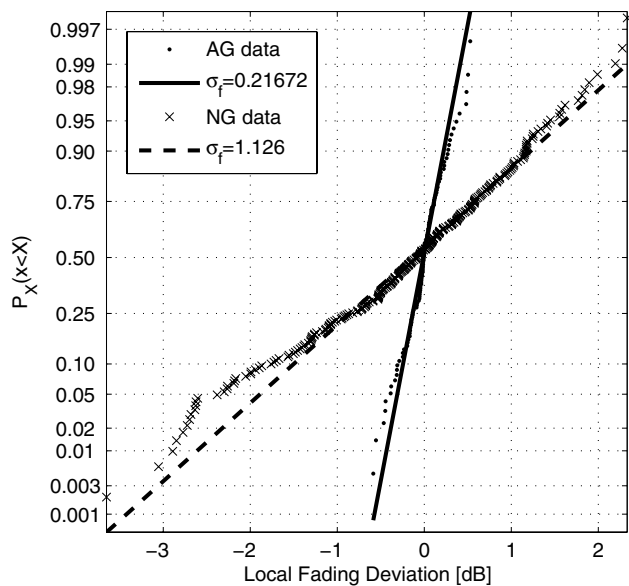
where β_k is a real number and the maximum value for τ_k is 50ns (it was observed that very little multipath energy existed beyond this excess delay). The multipath in the channel is characterized quantitatively by the first moment and the square root of the second central moment [5], which are referred to as the mean excess delay spread and the RMS delay spread, respectively, viz.,

$$\bar{\tau} = \frac{\sum_k \beta_k^2 \tau_k}{\sum_k \beta_k^2} \quad (6)$$

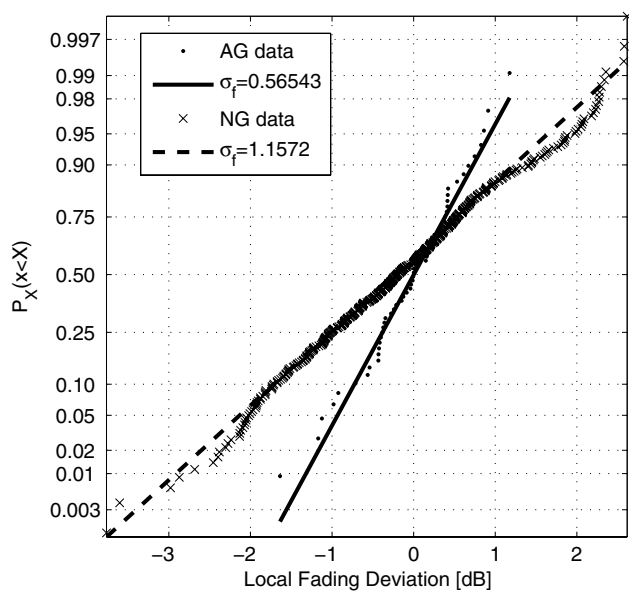
$$\tau_{rms} = \sqrt{\frac{\sum_k \beta_k^2 \tau_k^2}{\sum_k \beta_k^2} - \bar{\tau}^2} \quad (7)$$

Other valuable small scale statistics are the number of discrete paths (N_p) for the measured data (all nonzero elements of the CIR), and the Rake receiver performance. The Rake receiver ranks the discrete paths of the CIR, β_k from (5), in terms of energy; a common practice in wideband receiver design.

Mean excess delay spread, RMS delay, N_p , and Rake receiver performance are key statistics in developing channel models. For small scale channel modeling, this paper uses the Saleh-Valenzuela (SV) model, first proposed in [14] in 1987. Although the SV model was initially developed to describe NLOS channels—as it assumes clustering of rays—it is often used for LOS situations as well. Within the clusters, parameters $1/\lambda$ and γ describe the mean ray inter-arrival rate and exponential amplitude decay respectively of a Poisson process. The clusters themselves are also Poisson processes with respective parameters $1/\Lambda$ and Γ . Finally, the individual path amplitudes adopt a log-normal distribution with parameter σ about the expected power. Model parameters were calculated by curve-fitting Rake receiver performance and cumulative distribution functions for delay spread, mean excess delay, and number of paths in the minimum mean-square error sense and can be found in Table I.



(a) LOS



(b) NLOS

Fig. 5. Cumulative distributions of received power variations (local spatial fading).

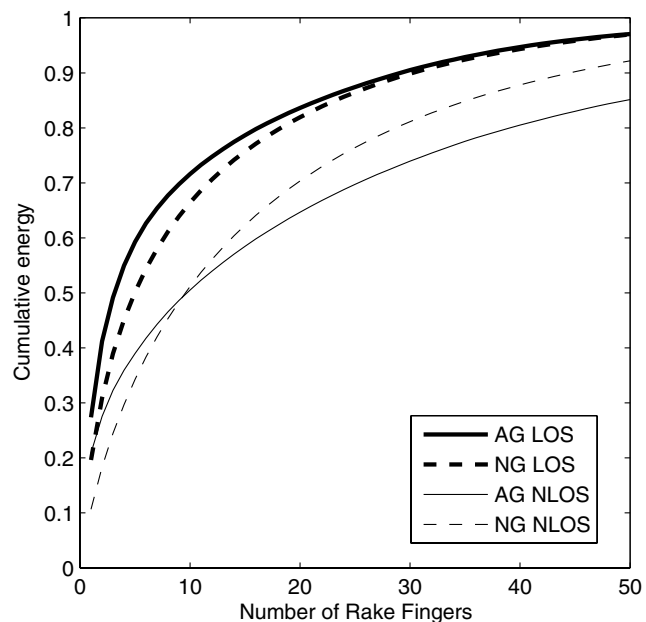


Fig. 6. Rake receiver performance; average accumulated energy for strongest 50 CIR paths, ranked in order of signal energy.

IV. RESULTS AND CONCLUSIONS

A total of 255 LOS and 393 NLOS power delay profiles were measured in a variety of locations and environments for evaluating the statistical properties of both large scale and small scale models. Above ground measurements were taken in the same buildings but in a previous measurement campaign using the exact same equipment and procedure as in the near-ground measurements.

The following observations have been made from Figures 2-7 and Tables I and II about the relationship between antenna height and channel statistics:

- 1) As demonstrated by Figure 2, lowering the antennas significantly decreases the amount of power seen at the receiver (particularly for the LOS component), even when Tx/Rx separation is small and can significantly degrade the performance of the system;
- 2) Figure 3 demonstrates the considerably higher path loss observed by placing the antennas directly on the ground than the free-space propagation, and nearly double that of above-ground. Furthermore, lowering the antennas significantly increases the shadowing variance;
- 3) For both LOS and NLOS situations, τ_{rms} and τ_m increase in both mean value and variance as antennas are lowered to the ground suggesting a larger dispersion of energy throughout the observation window (see Figure 7 and Table II);
- 4) Local spacial fading in Figure 5 also has a higher variation for NG than AG, particularly in the LOS case;
- 5) A more significant portion of the entire received energy is located in the strongest path (generally the LOS component) for AG measurements than for NG. This

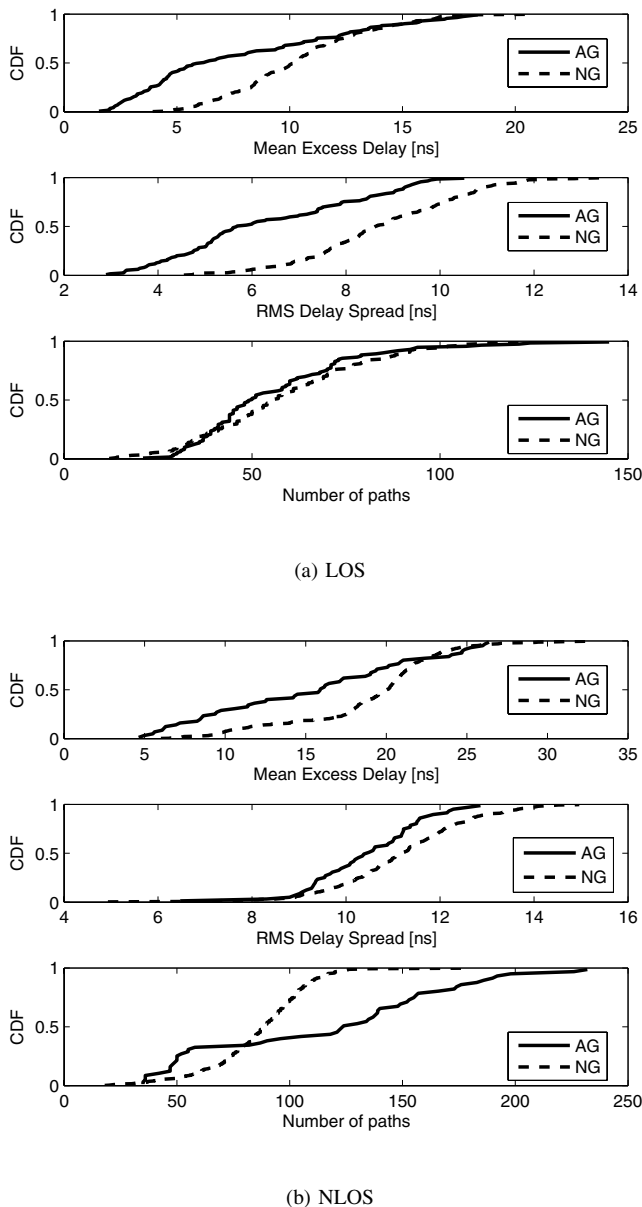


Fig. 7. Small scale statistics

is evident in Figure 6 as the strongest CIR component on average constitutes approximately 10% more energy in AG measurements than NG for both LOS and NLOS cases;

REFERENCES

- [1] K. Sohrabi, B. Manriquez, and G. Pottie, "Near ground wideband channel measurements," in *IEEE Transactions on Vehicular Technology*, vol. 1, May 1999, pp. 571–574.
- [2] Q. Li and W. S. Wong, "Measurement and analysis of the indoor uwb channel," in *IEEE Transactions on Vehicular Technology*, vol. 1, October 2003, pp. 1–5.
- [3] C. Chong, Y. Kim, and S. Lee, "Uwb indoor propagation channel measurements and data analysis in various types of high-rise apartments," in *IEEE Transactions on Vehicular Technology*, vol. 1, September 2004, pp. 150–4.

- [4] J. Karedal, S. Wyne, P. Almers, F. Tufvesson, and A. F. Molisch, "Uwb channel measurements in an industrial environment," in *IEEE GLOBECOM*, vol. 6, 29 Nov.-3 Dec. 2004, pp. 3511–6.
- [5] J. A. Dabin, N. Ni, A. M. Haimovich, E. Niver, and E. Grebel, "The effects of antenna directivity on path loss and multipath propagation in uwb indoor wireless channels," in *IEEE Conference on Ultra Wideband Systems and Technologies*, November 2003, pp. 305–9.
- [6] G. Durisi and G. Romano, "Simulation analysis and performance evaluation of an uwb system in indoor multipath channel," in *IEEE Conference on Ultra Wideband Systems and Technologies*, May 2002, pp. 255–8.
- [7] D. Cassioli, M. Win, and A. Molisch, "A statistical model for the uwb indoor channel," *IEEE Transactions on Communication*, 2001.
- [8] J. R. Foerster, "The effects of multipath interference on the performance of uwb systems in an indoor wireless channel," in *Vehicular Technology Conference*, vol. 2, May 2001, pp. 1176–80.
- [9] S. Promwong, J. ihi Tkada, P. Supanakoon, and P. Tangtisanon, "Theoretical ground reflection model for uwb communications systems," in *International Symposium on Communications and Information Technologies 2004*, October 2004, pp. 1208–12.
- [10] N. R. Adam, V. Atluri, and V. P. Janeja, "Poster on secure agency interoperation for border control and homeland security applications," in *2nd Symposium on Intelligence and Security Informatics*, June 10–11, 2004.
- [11] S. S. Ghassemzadeh, L. J. Greenstein, A. Kavčić, T. Sveinsson, and V. Tarokh, "UWB indoor path loss model for residential and commercial buildings," in *IEEE Vehicular Technology Conference*, vol. 5, October 2003, pp. 3115–9.
- [12] J. H. Reed, Ed., *An Introduction to Ultra Wideband Communications Systems*. Indiana: Prentice Hall, 2005.
- [13] F. Amoroso, "Effective bandwidth of DSPN signalling for mitigation of fading in dense scatterers," *Electronic Letters*, vol. 29, no. 8, April 1993.
- [14] A. Saleh and R. Valenzuela, "A statistical model for indoor multipath propagation," *IEEE Journal on Selected Areas in Communications*, vol. 5, no. 2, pp. 128–137, February 1987.